J|A|C|S
A R T I C L E S

Determination of Rate Constants for Charge Transfer and the Distribution of Semiconductor and Electrolyte Electronic Energy Levels in Dye-Sensitized Solar Cells by Open-Circuit Photovoltage Decay Method

Juan Bisquert,*,[†] Arie Zaban,*,[‡] Miri Greenshtein,[‡] and Iván Mora-Seró[†]

Contribution from the Departament de Ciències Experimentals, Universitat Jaume I, E-12080 Castelló, Spain, and Department of Chemistry, Bar-Ilan University, Ramat-Gan 52900, Israel

Received May 7, 2004; E-mail: bisquert@uji.es; zabana@mail.biu.ac.il

Abstract: A combination of electron lifetime measurement in nanoparticles as a function of the Fermi level position at high resolution in the potential scale with a new model to describe this dependence provides a powerful tool to study the microscopic processes and parameters governing recombination in dye-sensitized solar cells. This model predicts a behavior divided in three domains for the electron lifetime dependence on open-circuit voltage that is in excellent agreement with the experimental results: a constant lifetime at high photovoltage, related to free electrons; an exponential increase due to internal trapping and detrapping and an inverted parabola at low photovoltage that corresponds to the density of levels of acceptor electrolyte species, including the Marcus inverted region.

1. Introduction

There exists an increasing interest in obtaining a deeper understanding of the electronic and ionic processes that govern the operation of dye-sensitized solar cells (DSSC). One critical aspect of the solar cell toward larger conversion efficiency is the recombination of dye-photoinjected electrons into nanostructured TiO_2 with the redox species that regenerates the oxidized dye. Strategies based on purposeful control of the recombination properties, such as the core−shell nanoparticle approach,[1−3] could enhance significantly the efficiency of energy conversion of the DSSC. Many papers have addressed the kinetics of recombination of electrons in DSSC[4−11] (for a recent review see ref 12). In addition, the steady-state characteristics of DSSC (illumination dependence of the photovoltage) indicate a combination of mechanisms for interfacial charge transfer, involving direct transfer from conduction band, and also intermediate trapping at surface states with further charge transfer from the surface states to the isoenergetic acceptor levels.[13]

The lifetime of electrons in DSSC at different steady states of the solar cell is a particularly important quantity that was determined first by intensity modulated photovoltage spectroscopy (IMVS).[4,5] The measured lifetime, τ_n, is a strong function of the Fermi level or open-circuit photovoltage, V_{oc}. The lifetime is a kinetic quantity that contains information not only on the rate constants of charge transfer but also on the distribution of electronic states and electronic transitions that intervene in the operation of the DSSC.[14]

It was established that the general shape of $\tau_n(V_{oc})$ shows an exponential dependence.[4−6] This variation can be explained by classical arguments, based on electronic events occurring in the semiconductor material prior to carrier recombination, first provided by Rose, for amorphous photoconductors,[15] and recently adapted to DSSCs.[6,14] This model considers that the semiconductor contains a large number of electron traps and a low proportion of recombination centers. The measurement of the lifetime involves a determination of the time for the Fermi level to change about $k_B T$ (halving the electron density). But

[†] Universitat Jaume I.
[‡] Bar-Ilan University.
(1) Diamant, Y.; Chen, S. G.; Melamed, O.; Zaban, A. *J. Phys. Chem. B* **2003**, *107*, 1977.
(2) Palomares, E.; Clifford, J. N.; Haque, S. A.; Lutz, T.; Durrant, J. R. *J. Am. Chem. Soc.* **2003**, *125*, 475.
(3) Perera, V. P. S.; Pitigala, P. K. D. D. P.; Jayaweera, P. V. V.; Bandaranayake, K. M. P.; Tennakone, K. *J. Phys. Chem. B* **2003**, *107*, 13758.
(4) Schlichthörl, G.; Huang, S. Y.; Sprague, J.; Frank, A. J. *J. Phys. Chem. B* **1997**, *101*, 8141.
(5) Fisher, A. C.; Peter, L. M.; Ponomarev, E. A.; Walker, A. B.; Wijayantha, K. G. U. *J. Phys. Chem. B* **2000**, *104*, 949.
(6) Zaban, A.; Greenshtein, M.; Bisquert, J. *ChemPhysChem* **2003**, *4*, 859.
(7) Tachibana, Y.; Moser, J. E.; Grätzel, M.; Klug, D. R.; Durrant, J. R. *J. Phys. Chem.* **1996**, *100*, 200556.
(8) Kunciasuskas, D.; Freund, M. S.; Gray, H. B.; Winkler, J. R.; Lewis, N. *J. Phys. Chem. B* **2001**, *105*, 392.
(9) Willis, R. L.; Olson, C.; O'Regan, B.; Lutz, T.; Nelson, J.; Durrant, J. R. *J. Phys. Chem. B* **2002**, *106*, 7605.
(10) Kopidakis, N.; Benkstein, K. D.; van de Lagemaat, J.; Frank, A. J. *J. Phys. Chem. B* **2003**, *107*, 11307.
(11) Bauer, C.; Boschloo, G.; Mukhatar, E.; Hagfeldt, A. *J. Phys. Chem.* **2001**, *105*, 5585.

(12) Bisquert, J.; Cahen, D.; Hodes, G.; Rühle, S.; Zaban, A. *J. Phys. Chem. B* **2004**, *108*, 8106.
(13) Bisquert, J.; Zaban, A.; Salvador, P. *J. Phys. Chem. B* **2002**, *106*, 8774.
(14) Bisquert, J.; Vikhrenko, V. S. *J. Phys. Chem. B* **2004**, *108*, 2313.
(15) Rose, A. *Concepts in Photoconductivity and Allied Problems*; Interscience: New York, 1963.

all of the electrons in traps need to be anhillated through the recombination centers, requiring prior release to the conduction band. So the observed switching time, the *response time*, increases with respect to the lifetime of free electrons (determined by the rate of capture by the recombination centers), by the proportion of trapped to free electrons. This proportion changes exponentially as the Fermi level moves in the exponential distribution of states in the band gap.[15] It is noteworthy that the exponential dependence of $\tau_n(V_{oc})$ in DSSC is explained in this way assuming a *constant* rate of charge transfer (through conduction band states).[6,14]

Recently, we presented a general interpretation of the measured electron lifetime in DSSC as well as a new experimental method based on the treatment of open-circuit photovoltage decays (OCVD).[6] The OCVD technique is a method that consists of turning off the illumination in a steady state and monitoring the subsequent decay of photovoltage, V_{oc}. The response time is obtained by the reciprocal of the derivative of the decay curve normalized by the thermal voltage:

$$\tau_n = -\frac{k_B T}{e}\left(\frac{dV_{oc}}{dt}\right)^{-1} \tag{1}$$

This technique has the advantage with respect to alternative methods by small perturbation in frequency[4,5] or time domain[10] that OCVD provides as much resolution along the Fermi level axis as desired, in a single and fast measurement. Consequently, OCVD provides very detailed curves of $\tau_n(V_{oc})$ that contain a wealth of information on the electronic processes of recombination in DSSC, as we will show in this paper. It is important to note however that OCVD is basically a dark measurement of the solar cell. Consequently, recombination of the photoinjected electron with the oxidized dye, which is one of the two possible recombination paths, is not measured by OCVD. This phenomenon simplifies the interpretation of the results since only recombination to the electrolyte is measured. However one should take this into consideration when measuring cells in which regeneration of the dye is relatively slow as in the case of low redox concentrations or some of the solid-state mediators. In general, it must be recognized that recombination in DSSCs is a hierarchial process spanning many orders of magnitude in time. The OCVD is a quasi-equilibrium measurement that records the slow phenomena at characteristic times longer than ∼10 ms. Particularly for solar cells (that work at steady state), this is a very relevant range of time scales. Other, faster measurements by either time transients or high frequency domain provide information on the short time scale processes such as dye reduction or electron trapping in bulk. However in our case the kinetic behavior of these processes is not recorded, and they will not be considered in this work.

We will adopt an interpretation of the response time measured in DSSC by OCVD based on the electronic events in the semiconductor, followed by one-electron charge transfer, and this will be justified by the experimental results. A preliminary model presented previously describes electron trapping and detrapping in an exponential distribution in the bulk of semiconductor particles and further charge transfer by the conduction band mechanism, and this model suffices to explain major trends (the general exponential dependence) that are found in $\tau_n(V_{oc})$.[6,14] However, it is important to consider also the different routes for interfacial charge transfer, which change

significantly with the position of the Fermi level, due to the energy distribution of electronic states in both the semiconductor and the electrolyte.[13] It is therefore necessary to elaborate a complete model for the kinetic determination of lifetime as a function of steady state in quasi-equilibrium measurements that takes into account both the internal trapping and the combination of charge transfer routes. This will be done here for the first time. In particular, it will be shown by comparing the new model to a variety of experimental results that the Gaussian distribution of the effective electron acceptor levels in solution (according to Marcus-Gerischer transition rates) plays a major role in the shape of the lifetime. Important information on the global mechanism of charge-transfer in DSSC will be obtained. In addition, the importance of the results expands far beyond the specific system examined as they provide a new tool to study the electronic properties of nanoparticles in solution.

2. Theory

2.1. Basic Assumptions on Distribution of Electronic States and Rates of Charge Transfer. According to the previous works,[6,13,14] we formulate a model based on the assumption of several classes of electronic states in TiO$_2$ nanoparticles in a DSSC, as indicated in Figure 1. An important issue for the interpretation of kinetic measurements in DSSC is the possible need for a distinction between bulk traps and surface states. This issue is not clear from the previous work in the literature, but the necessity of these two kinds of states will be confirmed later on by our experimental results, and furthermore the respective parameters for the distributions will be obtained. Therefore we assume in the model the following:

(a) Conduction band states (or transport states or extended states). These have the property that they allow fast transport of the electrons. They are defined by the energy level E_c (lower edge of conduction band or mobility edge) and the effective density N_c. The volume concentration of electrons in these states relates to the quasi-Fermi level, E_F, as

$$n_c = N_c e^{(E_F - E_c)/k_B T} \tag{2}$$

provided that E_F is below the conduction band (nondegeneracy).

(b) The bulk traps. These are localized electronic states in the band gap that trap and release electrons only with the conduction band. The density of these states as a function of energy is described by the exponential distribution with a characteristic parameter T_0

$$g_b(E) = \frac{N_b}{k_B T_0}\exp[(E - E_c)/k_B T_0] \tag{3}$$

where N_b is the total density of bulk traps per unit volume. The volume concentration of electrons per unit energy at the energy E is given by $g_b(E) f_b(E, E_F)$, where $0 \le f_b(E, E_F) \le 1$ is the occupancy of bulk traps at this energy level. At quasi-equilibrium f is given by the Fermi−Dirac distribution at room temperature.

(c) The surface traps. These are localized electronic states in the band gap that are able to trap and release electrons with the conduction band and in addition are able to transfer electrons to the acceptor species in solution. These states are physically located either at the nanoparticle surface or within a tunneling
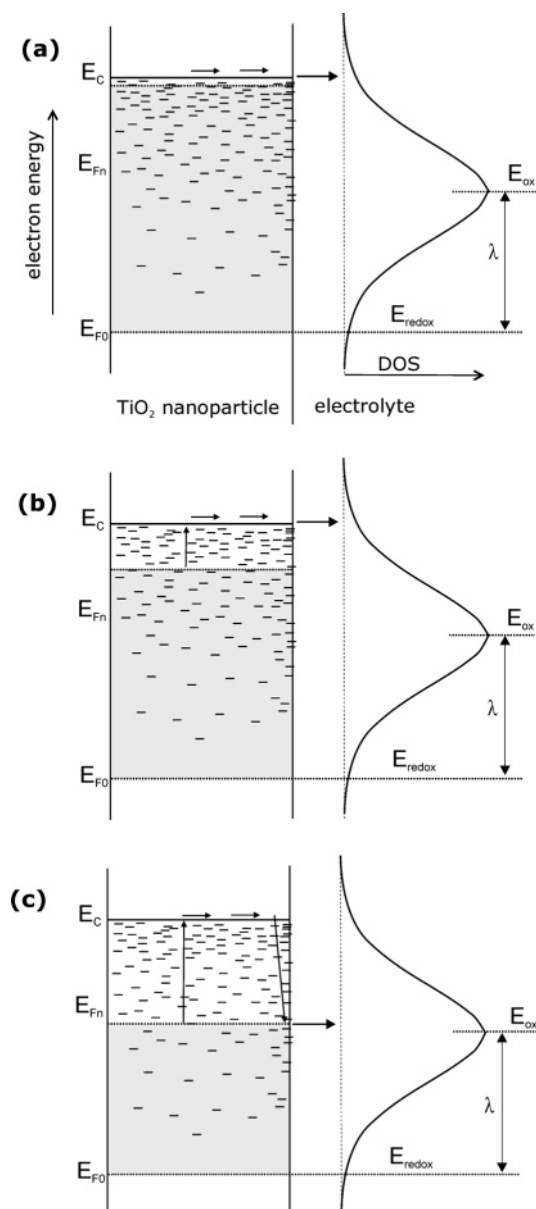
Figure 1. Schematics of the steps involved in the recombination of electrons in TiO₂ semiconductor nanoparticles during photovoltage decay, by charge transfer to the fluctuating energy levels in solution, which form a distribution with an effective Gaussian density of states (DOS), indicated at the right, with halfwidth λ, the reorganization energy, and peak at E_{ox}. E_{F0} shows the position of the Fermi level in the dark, which is equilibrated with the redox potential (E_{redox}) of the oxidized dye. (E_{Fn}) is the quasi-Fermi level of electrons at different stages of the photovoltage decay, and E_C is the conduction band energy. The shaded region indicates the band gap states that are occupied with electrons. (a) Transfer of conduction band electrons. (b) Transfer of electrons in traps, through conduction band, after thermal detrapping to the conduction band. (c) Transfer of electrons in traps, through surface traps, after thermal detrapping to the conduction band and capture by the surface trap.

distance from it. We assume also an exponential distribution with a characteristic parameter T_1

$$g_s(E) = \frac{N_s}{k_B T_1} \exp[(E - E_c)/k_B T_1] \qquad (4)$$

where N_s is the total density of surface traps per unit volume. The volume concentration of electrons per unit energy at the

energy E is given by $g_s(E) f_s(E,E_F)$, where $f_s(E,E_F)$ is the occupancy of surface traps at this energy level. The total density of localized states is given by $N_L = N_b + N_s$.

As mentioned before here we attempt to develop a complete model, in the sense that it is able to describe all the experimental features of kinetic results of lifetime in DSSC in quasi-equilibrium conditions at different steady states (as mentioned before the kinetic effects of the fastest processes occurring in the DSSC before it attains quasi-equilibrium are not considered). Recent calculations that will be reported elsewhere indicate that the demarcation level[13] for surface states is close to the redox level. Therefore we have assumed that quasi-equilibrium condition[14] for quasi-Fermi levels is obeyed during decays, meaning that electrons in traps remain in equilibrium with conduction band electrons, so that the occupancies of all the electronic states in the semiconductor ($f_b(E,E_F), f_s(E,E_F)$) are described by a single electron quasi-Fermi level, E_F, which in particular is the free electrons Fermi level that is monitored externally as a photovoltage, $V_{oc} = -(E_F - E_{F0})/e$. A deeper monoenergetic surface state situated close to the redox level E_{redox} is observed by other methods and is likely to depart from quasi-equilibrium, but the effect of this trap is not very significant to our results by the OCVD technique, so it has been generally neglected in this paper.

The change of electron density under a small variation of the Fermi level is described by the chemical capacitance,[16] which takes the following forms. For conduction band states

$$C_\mu^{(cb)} = e^2 \frac{\partial n_c}{\partial E_F} = e^2 \frac{n_c}{k_B T} \qquad (5)$$

for bulk traps

$$C_\mu^{(bt)} = e^2 \frac{\partial}{\partial E_F} \int_{E_v}^{E_c} g_b(E) f_b(E,E_F) \, dE \approx e^2 g_b(E_F) \qquad (6)$$

and for surface traps

$$C_\mu^{(st)} = e^2 \frac{\partial}{\partial E_F} \int_{E_v}^{E_c} g_s(E) f_s(E,E_F) \, dE \approx e^2 g_s(E_F) \qquad (7)$$

The last equalities of eqs 6 and 7 use the zero-temperature approximation of the Fermi–Dirac distribution.[16] Note that the capacitances C_μ in eqs 5–7 show an exponential dependence on the Fermi level. From quasi-equilibrium condition it is understood in the expressions below that all the capacitances $C_\mu^{(i)}$ are taken at E_F.

The rates of transfer of electrons from the semiconductor to the oxidized species in solution constitute an important element in the model that establishes the time scale of the response through the rate constants. The rates of transfer consist on the product of the electron concentration in the particular semiconductor state and a transition probability. The rate of transfer from surface traps at the energy level E is

$$r_{ox}^{(st)}(E) = g_s(E) f_s(E,E_F) e_{ox}^{(st)}(E) \qquad (8)$$

For conduction band states

$$r_{ox}^{(cb)} = n_c e_{ox}^{(cb)}(E_c) \qquad (9)$$

The transition probabilities, $e_{ox}^{(i)}$, where $i = $ (st, cb), are determined by the rate constant for isoenergetic electron transfer, $k_t^{(i)}$, and the probability densities of the fluctuating energy levels in solution, given by Marcus−Gerischer model for electron transfer:

$$e_{ox}^{(i)}(E) = 2k_B T k_t^{(i)} \frac{c_{ox}}{\sqrt{4\pi\lambda k_B T}} \exp\left[-\frac{(E - E_{ox})^2}{4\lambda k_B T}\right] \quad (10)$$

where c_{ox} is the concentration of electrolyte oxidized species, E_{ox} is the most probable energy level for the oxidized species, and λ is the reorganization energy. We will allow for different rate constants for transfer from conduction band states, $k_t^{(cb)}$, and surface traps, $k_t^{(st)}$, in $e_{ox}^{(cb)}$ and $e_{ox}^{(st)}$, respectively.

In contrast to the surface traps, which are distributed in energy, the transfer of conduction band electrons occurs in all conditions between the same energy levels (assuming that the band edges are pinned), and it defines a constant lifetime given by the expression

$$\tau_{cb} = \frac{1}{e_{ox}^{(cb)}(E_c)} \quad (11)$$

2.2. Derivation of the Lifetime. The response time is defined as the decay time in a small variation of the Fermi level, which can be written $E_F + \varphi_n(t)$, where E_F is the steady-state value and the time-dependent part is $\varphi_n < k_B T$. The relationship between n_c and the Fermi level

$$n_c(t) = n_c(E_F + \varphi_n) \quad (12)$$

gives, by expanding to first-order,

$$n_c(t) = n_c + \frac{\partial n_c}{\partial E_F}\varphi_n \quad (13)$$

The evolution of $\varphi_n(t)$ in eq 13 obeys a linear differential equation that defines the response time, as follows

$$\frac{\partial \varphi_n}{\partial t} = -\frac{\varphi_n}{\tau_n} \quad (14)$$

where τ_n is a function of the steady-state quasi-Fermi level and the parameters in the model. The specific decay equation, to be compared with eq 14, is obtained by linearizing the kinetic equations of the general model for trapping, detrapping and charge transfer, as shown in the following.

The equation of conservation for conduction band electrons contains three terms: the total rate for trapping and release in the distribution of bulk traps, the total rate of trapping and release in the distribution of surface traps, and the rate of transfer from conduction band to acceptor levels in solution, eq 9,

$$\frac{\partial n_c}{\partial t} = -\int_{E_v}^{E_c} \{\beta_b(E)n_c[1 - f_b(E)] - g_b(E)\,\epsilon_b(E)\,f_b(E)\}\,dE - \int_{E_v}^{E_c} \{\beta_s(E)n_c[1 - f_s(E)] - g_s(E)\epsilon_s(E)f_s(E)\}\,dE - r_{ox}^{(cb)} \quad (15)$$

The quantities $\epsilon(E)$ and $\beta(E)$ are rate constants for trapping and release at the energy level E.

The equation of conservation for bulk traps at the energy level E describes the only mechanism of exchange that is possible for these traps, the trapping and release from conduction band states

$$g_b(E)\frac{\partial f_b(E)}{\partial t} = \beta_b(E)\,n_c[1 - f_b(E)] - g_b(E)\,\epsilon_b(E)\,f_b(E) \quad (16)$$

Finally, the equation of conservation for surface traps at the energy level E contains both the trapping and release terms and the rate of transfer from that level to the electrolyte oxidized species at the same energy, eq 8,

$$g_s(E)\frac{\partial f_s(E)}{\partial t} = \beta_s(E)\,n_c[1 - f_s(E)] - $$
$$g_s(E)\,\epsilon_s(E)\,f_s(E) - r_{ox}^{(st)}(E) \quad (17)$$

Integrating eqs 16 and 17 and substituting in 15 we obtain

$$\frac{\partial}{\partial t}\{n_c + \int_{E_v}^{E_c} g_b(E)f_b(E)dE + \int_{E_v}^{E_c} g_s(E)f_s(E)dE\} = $$
$$-\frac{n_c}{\tau_{cb}} - \int_{E_{redox}}^{E_F} g_s(E)e_{ox}(E)dE \quad (18)$$

In the last term of eq 18 it has been assumed that $f_s(E)$ is described by a step function at quasi-Fermi level, E_F (i.e., only the surface traps below E_F participate in the charge-transfer process). One has from eq 13

$$\frac{\partial n_c}{\partial t} = \frac{\partial n_c}{\partial E_F}\frac{\partial \varphi_n}{\partial t} \quad (19)$$

and the terms in eq 18 can be linearized in the following way

$$\left[\frac{\partial n_c}{\partial E_F} + g_b(E_F) + g_s(E_F)\right]\frac{\partial \varphi_n}{\partial t} = $$
$$-\left[\frac{\partial n_c}{\partial E_F}\frac{1}{\tau_{cb}} + g_s(E_F)e_{ox}(E_F)\right]\varphi_n \quad (20)$$

which can be written also in terms of the chemical capacitances of eqs 5−7 as

$$[C_\mu^{(cb)} + C_\mu^{(bt)} + C_\mu^{(st)}]\frac{\partial \varphi_n}{\partial t} = $$
$$-\left[C_\mu^{(cb)}\frac{1}{\tau_{cb}} + C_\mu^{(st)}\,e_{ox}(E_F)\right]\varphi_n \quad (21)$$

By comparison of eqs 14 and 21, we obtain the final result for the response time:

$$\tau_n = \frac{C_\mu^{(cb)} + C_\mu^{(bt)} + C_\mu^{(st)}}{C_\mu^{(cb)}\tau_{cb}^{-1} + C_\mu^{(st)}\,e_{ox}^{(st)}(E_F)} \quad (22)$$

2.3. Interpretation and Shape of the Lifetime. We discuss here the structure of the result in eq 22. The numerator is the total chemical capacitance. In other words the total number of electrons that will have to be withdrawn from the semiconductor per dE_F, the small decrease of Fermi level implicit in the definition of the response time. Therefore the numerator contains all the possible kinds of electronic states, and this is because all of them are affected by the change of Fermi level.
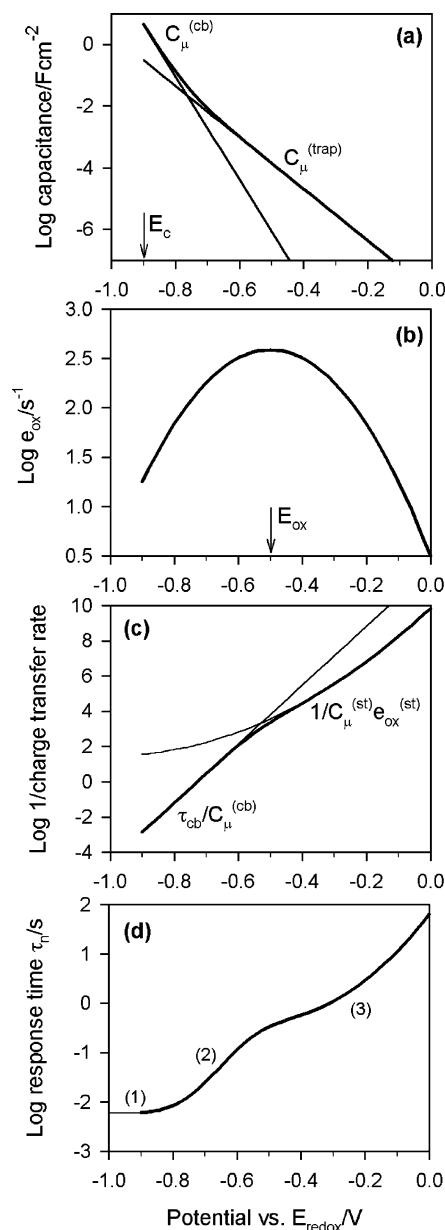
Figure 2. Representation of the response time in a DSSC as a function of open-circuit voltage and several associated quantities. The DSSC simulation parameters are as follows: $T = 300$ K, $L = 10\ \mu$m, $E_c = 0.9$ eV vs E_{redox}, $N_c = 6.8 \times 10^{20}$ cm^{-3}, $N_b = 1 \times 10^{20}$ cm^{-3}, $N_s = 5 \times 10^{17}$ cm^{-3}, $T_0 = T_1 = 600$ K, $c_{ox} = 3 \times 10^{19}$ cm^{-3}, $k_t^{(cb)} = 1 \times 10^{-15}$ cm^3 s^{-1}, $k_t^{(st)} = 1 \times 10^{-16}$ cm^3 s^{-1}, $\lambda = 0.50$ eV. (a) Chemical capacitance. The thin lines indicate the conduction band and trap contributions separately. (b) Probability of isoenergetic electron transfer to the electronic levels of oxidized species in solution. (c) The inverse of charge transfer rates, for both conduction band and surface traps transfer mechanisms, and total charge transfer resistance in thick line. (d) The response time.

The denominator of eq 22 contains a sum of differential rates of charge transfer, per dE_F, so there appears the number of electrons through the chemical capacitance times the probability of transfer. Each term contains only the chemical capacitance of those specific states that realize the charge transfer. In addition, each term contains the density of acceptor levels in solution and the rate constant for the charge transfer.

To discuss further the implications of the model we present simulation results in Figures 2−5. For the moment, and for clarity of discussion, we simplify the model assuming the same
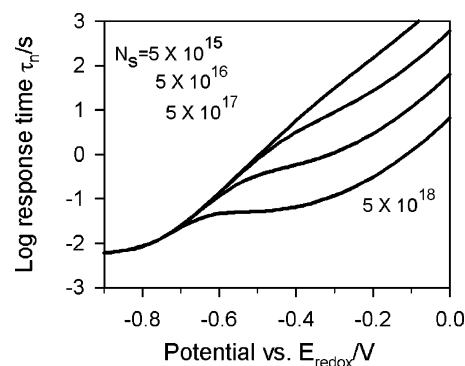

Figure 3. Representation of the response time in a DSSC as a function of open-circuit voltage. The DSSC simulation parameters are the same as those in Figure 2, and the surface trap density is varied as indicated in cm^{-3}.
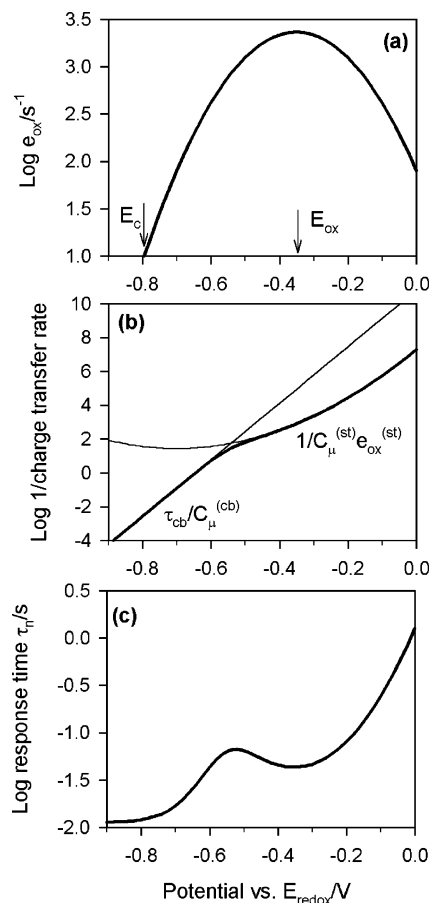

Figure 4. Representation of the response time in a DSSC as a function of open-circuit voltage. The DSSC simulation parameters are as follows: $T = 300$ K, $L = 10\ \mu$m, $E_c = 0.8$ eV vs E_{redox}, $N_c = 6.8 \times 10^{20}$ cm^{-3}, $N_b = 1 \times 10^{20}$ cm^{-3}, $N_s = 1 \times 10^{18}$ cm^{-3}, $T_0 = T_1 = 600$ K, $c_{ox} = 3 \times 10^{19}$ cm^{-3}, $k_t^{(cb)} = 5 \times 10^{-15}$ cm^3 s^{-1}, $k_t^{(st)} = 5 \times 10^{-16}$ cm^3 s^{-1}, $\lambda = 0.35$ eV. (a) Probability of isoenergetic electron transfer to the electronic levels of oxidized species in solution. (b) The inverse of charge transfer rates, for both conduction band and surface traps transfer mechanisms, and total charge transfer resistance in thick line. (c) The response time.

tailing parameters $T_0 = T_1$ for both bulk and surface traps. This restriction will be dropped later on.

Let us consider first some preliminary points about the density of electronic states and the rates of charge transfer. Figure 2a shows the expected behavior of the chemical capacitance.[16] When the Fermi level is low (more positive poten-

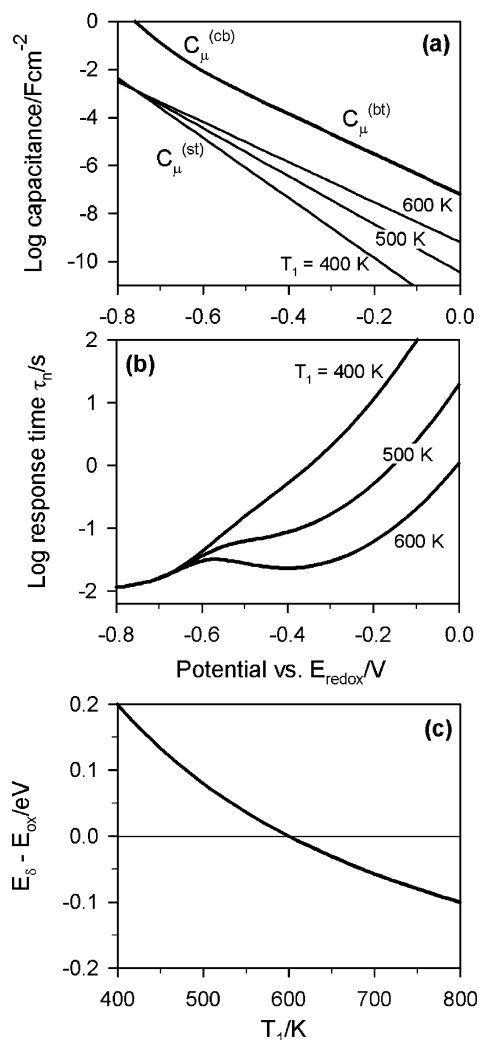(16) Bisquert, J. *Phys. Chem. Chem. Phys.* **2003**, *5*, 5360.

Figure 5. Representation of the response time in a DSSC as a function of open-circuit voltage and several associated quantities. The DSSC simulation parameters are as follows: $T = 300$ K, $L = 10$ μm, $E_c = 0.8$ eV vs E_{redox}, $N_c = 6.8 \times 10^{20}$ cm^{-3}, $N_b = 1 \times 10^{20}$ cm^{-3}, $N_s = 1 \times 10^{18}$ cm^{-3}, $T_0 = 600$ K, $c_{ox} = 3 \times 10^{19}$ cm^{-3}, $k_t^{(cb)} = k_t^{(st)} = 1 \times 10^{-15}$ cm^3 s^{-1}, $\lambda = 0.40$ eV. The characteristic temperature of the surface trap density, T_1, varies as indicated. (a) Chemical capacitance. The thick line is the total capacitance, showing the regions dominated by conduction band and bulk traps capacitance. The thin lines indicate the surface trap capacitance. (b) The response time. (c) Variation of the apparent oxidation energy, as estimated from the local minimum of the response time in the surface traps-dominated region, as a function of the characteristic temperature of the surface traps, for a bulk trap distribution with $T_0 = 600$ K.

tials), it is dominated by the bulk trap's capacitance (assuming $N_b \gg N_s$, as justified below)

$$C_\mu^{(trap)} = e^2 \frac{N_L}{k_B T_0} e^{(E_F - E_c)/k_B T_0} \qquad (23)$$

and by the conduction band capacitance, eq 5, when the Fermi level is close to the lower edge of the conduction band.

Figure 2b shows the probability of transfer from a given energy level to the corresponding acceptor states in solution. These are distributed as a Gaussian with a peak at E_{ox}, which is situated a distance λ above $E_{redox} = E_{F0}$. Therefore, assuming that the bands are pinned, the maximum rate for charge transfer from surface traps occurs at the level E_{ox}, which is the point of barrierless activation, where the Fermi level is when $V_{oc} = -\lambda/e$.

Another essential quantity determining the lifetime is the differential rate of charge transfer. The reciprocal of this rate is shown in Figure 2c, corresponding to the charge transfer resistance that can be measured by impedance spectroscopy.[17] More specifically, Figure 2c shows the reciprocal of the two terms in the denominator of eq 22, $C_\mu^{(cb)}\tau_{cb}^{-1}$ and $C_\mu^{(st)} e_{ox}(E_F)$, the larger of which dominates the charge transfer rate. Note that the probability e_{ox} is variable for surface traps, while it is constant (τ_{cb}^{-1}) for the conduction band states, so both terms display different dependences with the potential. The density of states in the conduction band is very large, and so when the Fermi level is very high, the rate of conduction band transfer becomes much larger than through the traps. The onset of the prevalence of direct transfer from conduction band is further discussed below.

The response time resulting from the elements that have been discussed is shown in Figure 2d. τ_n shows in this example three distinct regimes of behavior. Each of them corresponds to the processes outlined in the correspondent panels of Figure 1, as explained in the following:

(1) At high E_F the response time is constant. It can be seen in Figure 2a that $C_\mu^{(cb)} \gg C_\mu^{(traps)}$ and in Figure 2c that $C_\mu^{(cb)}\tau_{cb}^{-1} \gg C_\mu^{(st)} e_{ox}^{(st)}(E_F)$. Therefore eq 15 reduces to

$$\tau_n = \tau_{cb} \qquad (24)$$

In this regime one observes the lifetime of the free electrons in the conduction band, which is a constant, eq 11, without interference from trap effects (Figure 1a).

(2) At $E_F < 0.7$ eV in Figure 2d the response time increases linearly (in the log-linear representation). This occurs in the domain at which still charge transfer is dominated by the conduction band states, $C_\mu^{(cb)}\tau_{cb}^{-1} \gg C_\mu^{(st)} e_{ox}(E_F)$, but in which the trap capacitance becomes larger than the conduction band capacitance, $C_\mu^{(cb)} < C_\mu^{(traps)}$. From eq 22 we obtain in this case

$$\tau_n = \frac{C_\mu^{(trap)}}{C_\mu^{(cb)}}\tau_{cb} \qquad (25)$$

In this domain the response time dependence on the Fermi level is governed entirely by trapping and detrapping (Figure 1b).[6,14] (We remark however that trapping and detrapping time constants are not resolved separately, due to quasi-equilibrium conditions, but their ratio is described by the ratio of chemical capacitances in eq 25.) The slope of the line is determined by the tailing parameter T_0, as shown by the expression that is obtained from eqs 5, 23, and 25:

$$\tau_n = \frac{N_L T}{N_c T_0} e^{(T/T_0 - 1)(E_F - E_c)/k_B T}\tau_{cb} \qquad (26)$$

(3) In the region of lower V_{oc} values of Figure 2d the linear dependence turns into a curved one. This is when the charge-transfer process is governed by the distribution of surface traps, $C_\mu^{(cb)}\tau_{cb}^{-1} < C_\mu^{(st)}e_{ox}(E_F)$ (Figure 1c). Here $C_\mu^{(cb)} < C_\mu^{(traps)}$; hence eq 22 simplifies as follows

(17) Fabregat-Santiago, F.; Garcia-Belmonte, G.; Bisquert, J.; Zaban, A.; Salvador, P. *J. Phys. Chem. B* **2002**, *106*, 334.

$$\tau_n = \frac{C_\mu^{(\text{traps})}}{C_\mu^{(\text{st})} e_{\text{ox}}^{(\text{st})}(E_{\text{F}})} \qquad (27)$$

and we obtain the result

$$\tau_n = \frac{N_{\text{L}}}{N_{\text{s}}} \frac{1}{e_{\text{ox}}^{(\text{st})}(E_{\text{F}})} \qquad (28)$$

where the Fermi-level dependence of τ_n reveals directly the (reciprocal of) probability distribution in energy of the effective oxidized levels in solution. Hence the response time in log-linear plot shows in this domain a parabollic shape determined mainly by the value of the reorganization energy, λ. Equation 28 also contains as a prefactor the proportion of surface traps to bulk traps. This is because the electrons in the bulk traps have to be finally discharged from the semiconductor through the surface traps, which act in this case as the recombination centers. However, in contrast to eq 25, this factor $N_{\text{L}}/N_{\text{s}}$ does not imply in eq 28 a Fermi-level dependence, due to the assumption of identical distributions in bulk and surface. Below we show that, for *distinct* distributions, the shape of the lifetime in this domain is still the reciprocal of the Gaussian.

The energy level $E = E_{\text{F}}$ at which $C_\mu^{(\text{cb})}\tau_{\text{cb}}^{-1} = C_\mu^{(\text{st})}e_{\text{ox}}^{(\text{st})}(E_{\text{F}})$ is the transition from conduction band to surface states dominant charge transfer. This point is observed in the plots of τ_n as the change from the linear to the parabollic shape of the response time. Figure 3 shows the effect of moving this intersection point to more positive potentials by modifying the surface traps number and consequently the strength of surface states charge transfer. At the lowest surface trap density, $\log(\tau_n)$ displays a nearly linear dependence with V_{oc} which corresponds to the dominance of regime (2) up to low photovoltage. In contrast, by increasing the trap density, we eventually obtain that the intersection $C_\mu^{(\text{cb})}\tau_{\text{cb}}^{-1} = C_\mu^{(\text{st})}e_{\text{ox}}^{(\text{st})}(E_{\text{F}})$ occurs at an energy level above E_{ox}. Then, the response time presents a behavior which at first seems peculiar, with a local minimum, but then it is recognized as an implication of the Marcus inverted region. When the Fermi level moves through the surface states distribution, it scans the different values of the transition probablities $e_{\text{ox}}^{(\text{st})}$, which are governed by the effective density of states of acceptor levels in solution. This is shown more clearly in Figure 4 using a lower reorganization energy than those in the previous examples. Hence E_{ox} is closer to E_{redox}, so that the minimum is unmasked by regime 2, and Figure 4c shows directly the complete parabollic shape of the fluctuating energy levels in solution.

2.4. Diferent Distributions of Surface and Bulk Traps. As mentioned before, it is important to study the potential consequences for our measurements of different distributions of traps in bulk and surface. Let us discuss in more detail the region (3) of curved line shape, in the case in which the bulk and surface traps are characterized by different exponential distributions, $T_0 \neq T_1$ (this extension does not affect the features of regions 1 and 2 already discussed, provided that $N_{\text{s}} << N_{\text{L}}$, as expected for nanoparticles of size $\approx$ 15 nm). Instead of eq 28, we obtain from eq 27

$$\tau_n = \frac{g_{\text{b}}(E_{\text{F}})}{g_{\text{s}}(E_{\text{F}})e_{ox}^{(\text{st})}(E_{\text{F}})} \qquad (29)$$

therefore

$$\tau_n = \frac{N_{\text{b}}T_1\sqrt{4\pi\lambda k_{\text{B}}T}}{N_{\text{s}}T_0 2c_{\text{ox}}k_{\text{B}}Tk_{\text{t}}^{(\text{st})}} \exp\left[-\frac{E_{\text{F}} - E_{\text{c}}}{k_{\text{B}}T'} + \frac{(E_{\text{F}} - E_{\text{ox}})^2}{4\lambda k_{\text{B}}T}\right] \qquad (30)$$

where

$$\frac{1}{T'} = \frac{1}{T_1} - \frac{1}{T_0} \qquad (31)$$

which can be either positive or negative. Equation 30 can be written in the Gaussian form in the following way

$$\tau_n = \frac{N_{\text{b}}T_1\sqrt{4\pi\lambda k_{\text{B}}T}}{N_{\text{s}}T_0 2c_{\text{ox}}k_{\text{B}}Tk_{\text{t}}^{(\text{st})}} \exp\left[B + \frac{(E_{\text{F}} - E_\delta)^2}{4\lambda k_{\text{B}}T}\right] \qquad (32)$$

where

$$E_\delta = E_{\text{ox}} + \frac{2\lambda T}{T'} \qquad (33)$$

$$B = -\frac{\lambda T}{k_{\text{B}}T'^2} + \frac{1}{k_{\text{B}}T'}(E_{\text{c}} - E_{\text{ox}}) \qquad (34)$$

So when $T_0 \neq T_1$, the shape of $\tau_n(E_{\text{F}})$ in the domain controlled by surface traps is still a reciprocal of the Gaussian, but the minimum, at E_δ, is shifted with respect to E_{ox}.

The effect of the distribution of surface traps is shown in Figure 5. Note that, for the exponential distribution, the chemical capacitance $C_\mu^{(\text{st})}$ in Figure 5a shows directly the shape of the distribution of electronic states. Figure 5b shows that the tailing parameter for the surface traps T_1 has an enormous impact in the lifetime at low photovoltages; note that the number of surface traps is the same in all the examples. As the distribution becomes more shallow (decreasing T_1), the charge transfer through traps is reduced significantly. Although the traps become more concentrated in the energy levels near E_{c} at low T_1, this has no effect on the response time at high V_{oc} because here τ_n is dominated by conduction-band transfer. So the overall effect of reducing the depth of the exponential distribution of surface traps is similar to that of reducing the total number of surface traps, illustrated before in Figure 3. Additionally, the minima of the parabolla in Figure 5b shift with respect to E_{ox} toward negative potentials at decreasing T_1, and this is shown in more detail in the plot of eq 33 that is presented in Figure 5c.

3. Experimental Section

All chemicals were purchased from Aldrich Chemical Co. and used as received. Nanosize TiO_2 suspensions were synthesized using titanium tetraisopropoxide precursor. In brief, the titanium tetraisopropoxide dissolved at 1:1 ratio in 2-propanol was hydrolyzed by acetic acid pH 2 under rigorous stirring. After overnight aging, the 2-propanol was evaporated at 82 °C, and the suspension was autoclaved at 250 °C for 13 h resulting in 20 nm crystals. Conducting glass substrate, 8 ohm/square F-doped SnO_2 (Libby Owens Ford) was cleaned with soap, rinsed with deionized water (18.2 MΩ), and dried in air stream. The TiO_2 suspension was spread on the conducting substrate by a glass rod, using adhesive tapes as spacers. After the films were dried under ambient conditions, they were sintered in air at 450 °C for 30 min. The TiO_2 films thickness measured with a profilometer (Mitutoyo Co., Sueftest SV 500) was 4 μm.
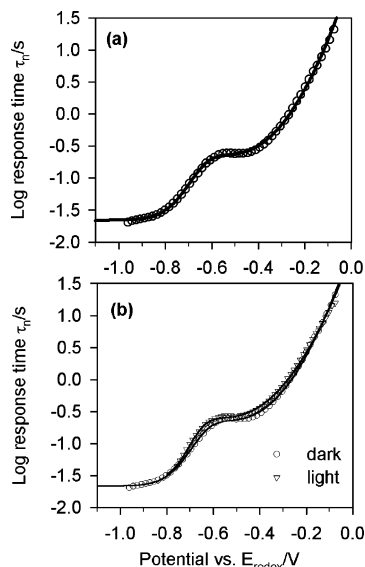
Figure 6. (a) Decay of the cell potential in a dye-sensitized solar cell with TBAI electrolyte following application of a negative bias (> -1.2 V) in the dark. (b) Comparison of the photovoltage decay (light) and the decay of the potential following an applied bias (dark). Lines correspond to the fits to the model discussed in the text. Parameters are given in columns 1 and 2 of Table 1.

The electrodes were sensitized by the N3 dye [*cis*-di(isothiocyanato)-bis(4,4-dicarboxy-2,2-bipyridine)ruthenium(II)] (Solaronic SA Co.). For dye adsorption the electrodes were immersed overnight in a 0.5 mM solution of dye in absolute ethanol. To avoid water, the films were heated to 120 °C before immersion in the dye solution.

A sandwich type configuration was employed to measure the performance of the dye-sensitized solar cell, using a F-doped SnO_2 film coated with Pt as a counter electrode. The distance between the two electrodes was fixed to 50 μm by two Teflon spacers. This spacing between the sensitized electrode substrate and the counter electrode that served also as a reference electrode is important for high reproducibility of the results in this thin cell configuration that lacks a real reference electrode. The electrolyte solution consisted of 0.5 M *tert*-butylammonium iodine (TBAI), 0.05 M I_2 in 1:1 acetonitrile/3-methyl-2-oxazolidinone (NMO). In the case of the Li^+ based electrolyte, 0.5 M LiI was used instead of the TBAI. Illumination of the cell was done with a 150 W Xe lamp calibrated to 1 sun.

For the photoinduced OCV decay measurements, the cell was illuminated to a steady voltage. The illumination was turned off using a shutter. The applied voltage decay and the open circuit photovoltage decay were recorded using an Ecochemie potentiostat equipped with a short interval sampling module. Typically the measurement interval was 10−50 ms. The OCVD analysis refers only to values measured after the shutter obtained full darkness.

Least-squares fitting of OCVD results was done with a specific code (available as Supporting Information) written for SigmaPlot software. The density of conduction band states was taken as $N_c = 6.8 \times 10^{20}$ cm^{-3}, and layer thickness, as $L = 10$ μm

4. Results and Discussion

Results of OCVD for DSSC with a TBA$^+$ cation in different conditions are presented in Figures 6 and 7. The results of the fits to the model are shown as lines, and the parameters listed in Table 1. The more complete curve $\tau_n(V_{oc})$, concerning the different regimes of behavior commented above, was obtained by applying a negative voltage and monitoring the subsequent decay in the dark and is shown in Figure 6a. By this method, it was possible to probe the response time up to very negative
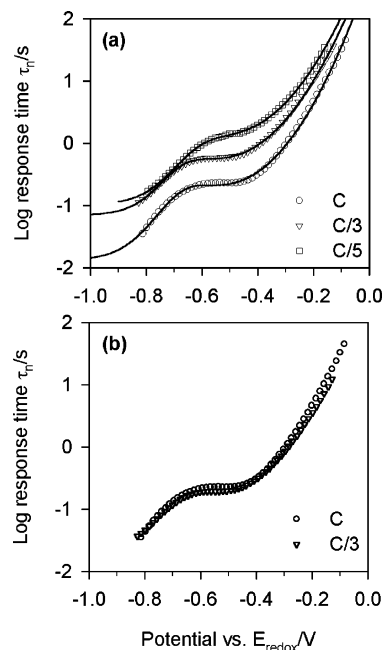

Figure 7. (a) Photovoltage decays of a single dye-sensitized solar cell with different concentrations of I_3^-, changing in the proportion indicated, with $c = 0.05$ M. Lines correspond to the fits to the model discussed in the text. Parameters are given in columns 3 to 5 of Table 1. (b) Rescaling of the data after dividing by 3 the data of τ_n for $c/3$.

open-circuit voltage, and the region 1 (Figure 2(d)) of nearly constant lifetime by predominance of direct transfer from conduction band states was detected. This region where the Fermi level is entering the conduction band cannot be reached by illumination, and so it was not found in the previous work.[6] A comparison between the photoinduced OCVD and the applied voltage decay is shown in Figure 6b. The figure confirms that both decays show nearly the same shape in the region where the former can be measured (from the maximum photovoltage ≈ 0.8 V). We can see in Figure 6 that, below 0.8 V, the lifetime begins to increase exponentially, corresponding to the domain 2 discussed before, where lifetime varies due to the change of the rate of trapping and detrapping, but still charge transfer is dominated by conduction band transfer. Finally, below 0.6 V the data display the parabollic shape that corresponds to the dominant transfer through surface states at the Fermi level. So Figure 6 displays all the features that were predicted in the model outlined in section 2 of this paper. In addition, the fits of the data in Figure 6 to the model, and also at varying concentrations of the electron acceptor, Figure 7, gave excellent agreement. The results show that the model developed previously estimates all the relevant aspects of the DSSC, concerning recombination process and the response time, that are recorded in the quasi-equilibrium measurement of OCVD.

Our results also establish OCVD as a technique with an enormous power of resolution for obtaining the microscopic parameters governing recombination in DSSCs. We have obtained from the fits eight independent parameters for recombination in DSSC: the densities and tailing parameters of both bulk and surface traps; the reorganization energy; the position of the conduction band with respect to the redox energy; and the rate constants for charge transfer both from conduction band and surface states. Depending on the detailedness of features of the curves, and the width of the potential window, some of

Table 1. Parameters for Distribution of Semiconductor and Electrolyte Electronic Energy Levels and Rate Constants for Charge Transfer in Dye Sensitized Solar Cells

cation	TBA+							Li+
data (curve)	dark (Figure 6)	light (Figure 6)	C_1 (Figure 7)	$C_2 = C_1/3$ (Figure 7)	$C_3 = C_1/5$ (Figure 7)	mean value[a]	reproducibility[b]	(Figure 8)
$\log_{10}(N_b/cm^{-3})$	20.0	19.7	20.8	20.4	20.2	20.2 ± 0.4	20.5 ± 0.5	19.7
$\log_{10}(N_s/cm^{-3})$	18.4	17.8	19.3	18.6	18.1	18	18.8 ± 0.2	17.8
T_0 (K)	587	828	523	544	515	599 ± 120	530 ± 30	802
T_1 (K)	446	674	354	391	388	450 ± 120	360 ± 50	600
λ (eV)	0.375	0.454	0.338	0.371	0.361	0.380 ± 0.040	0.33 ± 0.09	0.486
$E_c - E_{redox}$ (eV)	0.891	0.891^c	0.891^c	0.891^c	0.891^c	0.89	0.891^c	0.961
$A_{cb} = k_t^{(cb)}c_{ox}$ (s^{-1})	2.86×10^5	1.58×10^4	2.79×10^6	1.04×10^5	1.09×10^5		$(9 \pm 9) \times 10^7$	9.04×10^5
$A_{st} = k_t^{(st)}c_{ox}$ (s^{-1})	1.56×10^4	6.83×10^3	7.52×10^4	1.93×10^4	1.25×10^4		$(9 \pm 5) \times 10^5$	1.02×10^4
$k_t^{(cb)}$ (cm^3 s^{-1})^d	9.50×10^{-15}	5.24×10^{-16}	9.27×10^{-14}			1×10^{-14}		3.00×10^{-14}
$k_t^{(st)}$ (cm^3 s^{-1})^d	5.18×10^{-16}	2.27×10^{-16}	2.50×10^{-15}			1×10^{-15}		3.38×10^{-16}
$A_{cb}(C_1)/A_{cb}(C_x)$				26.8	25.5			
$A_{st}(C_1)/A_{st}(C_x)$				3.88	6.01			

^{a} Average of previous columns. ^{b} Average and standard error of 3 measurements at C_1 ^{c} Parameters fixed during fit. ^{d} Obtained using the value of A and $c_{ox} = 3.01 \times 10^{19}$ cm^{-3} [0.05 M].

the parameters are determined with high statistical confidence, while others less so. For the curve labeled TBA+ *dark* (see column 1 in Table 1), the confidence level > 99.99% is only attained by parameters T_0, T_1, and λ, and only by λ in the case of DSSC with Li+ (column 8). For the rest of the parameters, the standard errors obtained are of the same order as those of the parameter values. For the fits labeled TBA+ *light*, C_1, C_2, and C_3 (columns 2−5), the confidence level > 99.99% is attained by all the parameters except for $\log(N_s)$ and $k_t^{(cb)}$ (the $E_c - E_{redox}$ value has been prefixed in these cases). In this sense, the values found for these last parameters have to be taken as an estimation. In Table 1 the mean value and dispersion statistical error of the parameters of DSSC with TBA+ obtained with high confidence level by fitting are listed (column 6), while, for the other parameters, only the value order is indicated. In all cases the regression coefficient of fits is $r^2 > 0.998$. It was found necessary to use all the independent parameters enumerated above; for instance if the same tailing parameters $T_0 = T_1$ is considered in the fit, the r^2 diminish, while considering the same rate constant for transfer $k_t^{(st)} = k_t^{(cb)}$, the density of traps obtained is anomalously high.

Additionally, to confirm the reproducibility of results of this experimental method three independent measurements at concentration C_1 were performed in the same sensitized electrode. The different curves $\tau_n(V_{oc})$ are similar to that of Figure 6 and are practically overlaid so they are not shown. Each curve was fitted independently, and the mean values of parameters and their standard error obtained from the multiple measurement are reported in column 7 of Table 1. It can be seen that the dispersion of parameters is typically of 5−10%, which is a reliable accuracy for this photoelectrochemical experiment, except in the parameters A related to the rate constants for charge transfer, which are less resolved.

We discuss the main implications of the quantitative results obtained from the data. We remark that the simplification of the model to equal distribution of bulk and surface traps, $T_0 = T_1$, gives very poor fits, which indicates clearly that the surface states in nanostructured TiO$_2$ have different features than those of bulk traps. Bulk trap densities in the range 10^{20} cm^{-3} with an exponential distribution have been determined, with a tailing parameter $T_0 = 600$ K. The density of surface traps in the exponential distribution is 1/100 less than bulk traps, and for

particles of 10 nm radius, the number of surface traps is about 4 per particle. The surface state distribution appears to be much more shallow, with $T_1 = 450$, than the bulk traps. This is relevant for interpreting the curved low photovoltage region. Indeed, the minimum of the parabola that is observed in Figure 6 is displaced negatively 0.1 V from E_{ox}, according to Figure 5c. Therefore the E_{ox} level is at 0.38 eV vs E_{redox}, as confirmed by the fitting results in Table 1. This is the value of reorganization energy for I$_3^-$ in the presence of the TBA+ cation.

In the literature, there are alternative explanations for the lifetime dependence on Fermi level, based on a second-order dependence of the recombination rate on the acceptor concentration[4] or electron density.[5] So it is important to check the pressupositions adopted here where the recombination is clearly linear in both electron density (at the different kinds of semiconductor electronic states involved in the process) and acceptor concentration, eqs 8−10. First we note that the variation of the lifetime with the electron density in TiO$_2$ has been taken into account by our model which is in detailed agreement with the experimental results of $\tau_n(V_{oc})$. The reasons for the variation of the lifetime in this model, due to factors such as trapping and detrapping and distribution of the electronic states, have been discussed already. We remark that despite the linear kinetics of charge transfer the lifetime is not constant due to the thermodynamic prefactor in eq 25 and to the Marcus rate in eq 28. The conclusion that the rate of recombination is of first-order in electron concentration in each kind of state is in agreement with previous reports.[18]

In addition we have performed measurements of the lifetime for varying concentrations of the acceptor species while keeping constant the rest of the conditions of the solar cell, shown in Figure 7. The resulting parameters are given in Table 1. The results for the charge transfer parameter through surface traps, A_{st} (Table 1), show that the lifetime scales linearly with the acceptor concentration. Note that this parameter is determined for a wide window $\Delta V_{oc} \approx 0.5$ V, while the results for A_{cb} are affected by high uncertainty, as commented previously. Rescaling of the curves differing by a factor of 3 in acceptor concentration presented in Figure 7b shows that the two $\tau_n(V_{oc})$ curves nearly overlap. In contrast to this, the results of ref 4 by

(18) Haque, S. A.; Tachibana, Y.; Willis, R. L.; Moser, J. E.; Grätzel, M.; Klug, D. R.; Durrant, J. R. *J. Phys. Chem. B* **2000**, *104*, 538.

IMVS proposed a scaling of the type $\tau_n \propto c_{ox}^2$; however it is possible that these results have been influenced by a sideways shift of the $\tau_n(V_{oc})$ curves by the change of E_c due to the variation of the Li$^+$ concentration.

Having obtained detailed information from kinetic determination of the lifetime, we can now discuss the relative significance of the different routes for recombination at *steady state*, which is a central issue for the solar operation. From the previous analysis of the lifetime, it was concluded that the main recombination mechanism is a function of the Fermi level; at low V_{oc}, the surface traps dominate the transference, mainly due to a low ocupancy of the conduction band states, while the latter dominate at high photopotentials. In the working conditions of the solar cell, most of the TiO$_2$ nanostructure will be in a state of a high Fermi level. In principle the conduction band states must provide the main pathway for charge transfer, but all the surface traps are below the Fermi and also contribute to the recombination. Using the average parameters given in Table 1, we calculate the rate of electron transfer from TiO$_2$ to the acceptor ions, at the maximum photovoltage of 0.8 V. From eq 9, we obtain for the conduction band transfer $r_{ox}^{(cb)} = 8 \times 10^{17}$ cm^{-3} s^{-1}. The total contribution of the surface traps is given by

$$r_{ox}^{(st)} = \int_{E_{redox}}^{E_c} g_s(E) f_s(E, E_F) e_{ox}^{(st)}(E) \, dE \qquad (35)$$

and the integration gives $r_{ox}^{(st)} = 2 \times 10^{17}$ cm^{-3} s^{-1}. This result is important because it shows that the surface traps may provide a significant contribution (20% in our photoelectrodes) of the recombination losses. It follows that surface treatments that eliminate the effect of surface traps (this could be achieved, for example, by coating with ultrathin oxide layer[2]) may lead to a significant improvement of the conversion efficiency of the solar cell. It should also be remarked that the contribution of the surface traps is relatively much more significant at lower values of the Fermi level, when many surface states have a high probability of being occupied, while the free electron concentration is very low. For example, repeating the calculation at V_{oc} = 0.4 V, we obtain $r_{ox}^{(cb)} = 2 \times 10^{11}$ cm^{-3} s^{-1} and $r_{ox}^{(st)} = 9 \times 10^{16}$ cm^{-3} s^{-1}. So $r_{ox}^{(st)}$ is similar between 0.8 and 0.4 V open-circuit photovoltage at steady state, while $r_{ox}^{(cb)}$ decreases by 6 orders of magnitude.

It must be recognized that the effective Gaussian distribution of acceptor levels plays a dominant role in the recombination properties. Indeed from eq 11 it is found that the density of acceptor states at the conduction band level ($E_c = 0.89$ eV) is a fraction 4×10^{-6} of the density at the peak at $E_{ox} = 0.38$ eV (Figure 1). So while the recombination through conduction band states is favored by their much larger density and larger rate constant, the surface states contribution is large because they match much better the available acceptor levels. Thus the reorganization energy appears to be a crucial factor for controlling recombination in DSSC, especially for placing the transfer through conduction band deep into the Marcus inverted region. Besides the possibility of passivating the surface traps, we point out that it may be favorable to decrease the tailing parameter
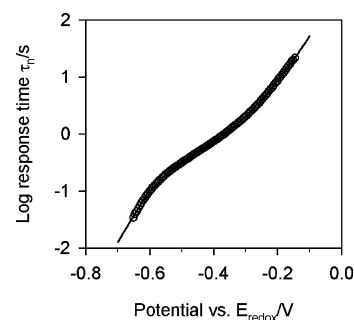

Figure 8. Comparison of the model results (thin line) with the measurement reported previously[6] of the response time in a DSSC with Li$^+$ cation by open-circuit photovoltage decay.

T_1 in order to remove the surface states from the region of high density of acceptor levels.

Finally, results of a DSSC with Li$^+$ cation reported previously[6] have been fitted to the model reported here and are presented in Figure 8 and the last column of Table 1. It is appreciated in Figure 8 that the data contain the regimes 2 and 3 of the lifetime, though not the stabilization of the lifetime at high Fermi level. The parabollic region of regime 3 (not discussed in the preliminary model given in ref 6) can now be appreciated. In Li$^+$ it is less visible than in the TBA$^+$ cation, due to the fact that the reorganization energy in Li$^+$ is larger, 0.48 eV, than that in TBA$^+$. More extensive characterization of DSSC with Li$^+$ cation by this method will be presented elsewhere.

5. Conclusions

A combination of electron lifetime measurement in nanoparticles as a function of the Fermi level position at high resolution in the potential scale, with a new model to describe this dependence, provides a powerful tool to study the electronic properties of nanoparticles in solution. We show that placing the nanoparticles on a conductive substrate allows extraction of eight parameters related to the electronic paths in the nanoparticles, the distribution of trapping states in the particles and rate constants for the electron reaction with electrolyte.

Regarding the specific system examined, the dye sensitized solar cell, we find three voltage dependent regions in which the lifetime is dominated by different factors: (1) a constant lifetime at high photovoltage, related to free electrons; (2) an exponential increase due to internal trapping and detrapping; and (3) an inverted parabolla at low photovoltage that corresponds to the reciprocal of the density of levels of acceptor electrolyte species, including the Marcus inverted region. The results provide guidelines for improvement of the performance of the dye cells.